Electronic measurement of femtosecond time delays for arbitrary-detuning asynchronous optical sampling

Laura Antonucci, Xavier Solinas, Adeline Bonvalet, Manuel Joffre

Electronic measurement of femtosecond time delays for arbitrary-detuning asynchronous optical sampling

Laura Antonucci*, Xavier Solinas, Adeline Bonvalet, Manuel Joffre
Laboratoire d'Optique et Biosciences
CNRS, INSERM, École Polytechnique, Institut Polytechnique de Paris
91128 Palaiseau, FRANCE

January 4, 2021

Abstract

Arbitrary-Detuning ASynchronous OPtical Sampling (ADASOPS) is a pump-probe technique which relies on the stability of femtosecond oscillators. It provides access to a multiscale time window ranging up to millisecond, combined with a sub-picosecond time resolution. In contrast with the first ADASOPS demonstration based on the interferometric detection of coincidences between optical pulses, we show here that the optical setup can now be reduced to a mere pair of photodetectors embedded in a specially-designed electronic system. In analogy with super-resolution methods used in optical microscopy for localizing single emitters beyond the diffraction limit, we demonstrate that purely electronic means allow the determination of time delays between each pump-probe pulse pair with a standard deviation as small as 200 fs. The new method is shown to be simpler, more versatile and more accurate than the coincidence-based approach.

1 Introduction

Ultrafast pump-probe spectroscopy is a very powerful technique for investigating a large number of systems in various fields such as photophysics, photochemistry or biochemistry. With this approach, the time-resolved dynamics of samples under study is typically accessed by varying the time delay between two ultrashort pulses which are respectively responsible for transient excitation (pump pulse) and for monitoring the system photonic response (probe pulse). A unique property of pump-probe spectroscopy lays in the fact that its time resolution is not ultimately limited by the photodetector response time but, depending on the methodological approach, can be reduced to the limit associated with the optical pulse duration. These different approaches also result in a broad variety of accessible time windows[1].

With regard to the measurement resolution, we can distinguish between two main categories: sub-picosecond and sub-nanosecond techniques. In conventional sub-picosecond techniques the delay between pump and probe pulses, or its law of evolution for consecutive pump-probe pulse pairs, is a predetermined parameter. For example, in the most widespread version of pump-probe spectroscopy the two beams originate from the split of a single laser beam, and their relative delay is mechanically controlled by varying the optical path difference with the use of a linear translation stage. In more elaborate techniques, such as asynchronous optical sampling (ASOPS) [2, 3, 4, 5, 6, 7], pump and probe beams originate from two different lasers, whose almost identical repetition rates are finely tuned in order to generate a suitable scanning rate. On the other hand, sub-nanosecond techniques are also based on two different lasers, but instead of assigning

*laura.antonucci@polytechnique.edu

a predetermined delay, the actual delay is measured *a posteriori* by electronic means [8], thus resulting in a poorer time resolution.

With regard to the accessible measurement window, the value of the speed of light confines the linear-stage technique to about ten nanoseconds at most. In contrast, the maximum delay achievable with the two-laser technique is limited only by the upper repetition period, which ranges typically between roughly 10 ns for oscillators and 1 ms for amplified systems. Alternatively, single pump pulse measurements with a continuous probe are also available [9, 10]. The most straightforward methods thus have to compromise between time resolution and time window, with either a sub-picosecond resolution over a nanosecond time window, or a sub-nanosecond resolution over a millisecond time window. However, there are numerous systems of interest, e.g. complex macromolecules[11, 12, 13, 14, 15, 16], which present rich dynamics with different time constants, so that multiscale approaches able to combine a large time window with a picosecond or sub-picosecond resolution are highly desirable. For this purpose, different alternative techniques have been developed, including, for example, the ASOPS method mentioned above[2, 3, 4, 5, 6, 7], or the combination of two amplified laser systems [17, 18, 19, 20, 21, 22]. The latter method, which allows access to a millisecond time window combined with a picosecond or sub-picosecond time resolution, relies either on two synchronized oscillators that can be phase shifted[17, 18], or on a single oscillator seeding both amplifiers with a mechanical delay line for controlling short-delay values[19, 20, 21, 22].

We have previously developed a specific ASOPS variant suitable for free-running oscillators of arbitrary repetition rates, hence coined Arbitrary Detuning ASOPS or simply ADASOPS[23]. Using this method, we managed to extend the typical 10-ns ASOPS measurement window to about 200 ns by using a long cavity oscillator for the pump laser [14]. More recently, we also combined this approach with kHz amplified laser systems. In this way, a 1-ms measurement window can be readily covered with a sub-picosecond time resolution [24], outweighing the limitations mentioned above. Furthermore, we highlighted how multiscale control and rapid scanning of time delays can thus be achieved [25]. In contrast with previous techniques, ADASOPS neither completely pre-assigns the delay nor purely measures it afterwards. ADASOPS relies rather on the great stability of femtosecond oscillators in order to accurately determine the actual law governing the time delay between all oscillator pulse pairs.

So far, the implementation of ADASOPS has been based on the optical detection of temporal coincidences between pump and probe pulses. Such a detection can be implemented by interferometric means, provided the laser spectra present a significant overlap[23]. However, the main drawback of such an implementation is its critical dependence on the coincidence rate. This can be detrimental when there is a significant drift of cavity lengths during the blind time interval between two coincidences, e.g. for oscillators embedded in an amplifier or for a low-repetition-rate oscillator. Indeed, temporal coincidences between femtosecond oscillators are relative rare events, occurring at a typical rate of approximately 1 kHz in the case of two 80-MHz femtosecond oscillators. Consequently, coincidence-based ADASOPS makes very precise snapshots of the system every millisecond on average and assumes that the delay evolves linearly during the blind interval between coincidences. Although the time resolution can be improved by selecting only coincidence pairs that happened to be close enough, this approach results in ignoring valuable data which is detrimental to the signal to noise ratio [24]. Although one could envision various methods for increasing the coincidence rate, for example by duplicating the coincidence detection stage for different time delays, this would result in an increased complexity of the optical setup.

In this article we present a different approach, hereafter referred to as optoelectronic ADASOPS, which is based on a high-rate electronic measurement of the delay between pump and probe pulses using a Time-to-Digital Converter (TDC), and the ensuing reconstruction of the time-delay law of evolution. Although the accuracy of each measurement is degraded by almost two orders of magnitude with respect to the detection of optical coincidences, this is more than compensated for by the large number of measurements thus made available. In some regard, our method can be seen as a time-domain analog of super-resolution optical

microscopy where a single emitter can be localized with an accuracy corresponding to the diffraction limit divided by $\sqrt{N}$, where N is the number of detected photons[26]. The same result holds true in our case, where N is now the number of measurements. We can thus expect a time resolution of the order of $R_{\mathrm{tdc}}/\sqrt{N}$, where the TDC time resolution, R_{tdc}, plays the same role as the diffraction limit in optical microscopy.

In the following, we first detail the principle of optoelectronic ADASOPS. We then characterize the time resolution of our electronic system and finally demonstrate the sub-picosecond time resolution of optoelectronic ADASOPS by direct comparison with the detection of optical coincidences.

2 Principle of optoelectronic ADASOPS

The basic principle of ADASOPS relies on the determination and regular update of the law of delay evolution between pump and probe pulses. This law can subsequently be used to accumulate measured data in appropriate time bins[14] or to decide which pulse to selectively amplify[25]. If we number each probe pulse with an integer i, the law of delay evolution can be approximated with the following expression of the time delay Δt_i elapsed since the previous pump pulse,

$$\Delta t_i = P_n(i)\ [T_1] = \sum_{k=0}^{n} p_k\, i^k\ [T_1], \tag{1}$$

with $P_n(i)$ being a degree-n polynomial function of i associated with real coefficients p_k, T_1 being the pump oscillator period and $[T_1]$ standing for the modulo-T_1 operation. If we call T_2 the probe oscillator period, a first-order polynomial with a slope p_1 equal to $(T_2 - T_1)[T_1] = T_2[T_1]$ would be appropriate in the case of two ideal oscillators. However, higher-order polynomials can be useful to account approximately for a drift in cavity lengths. In practice, the $n + 1$ coefficients p_k must be continuously updated in order to keep track of unavoidable fluctuations of the cavity lengths. In the coincidence-based version of ADASOPS, each new coincidence detection triggers an update of the coefficients of a linear – or sometimes quadratic – polynomial[23]. In optoelectronic ADASOPS, instead of making a small number of very accurate measurements of rare coincidence events, we acquire a much greater number of less-accurate measurements. This is achieved by generating two electronic signals from pump and probe pulse trains and measuring the delays using a TDC with a time resolution of the order of 10 ps. Measurements are repeated at a given frequency, of the order of 10 MHz as limited by the TDC specifications. The $n + 1$ coefficients of polynomial P_n are then determined by applying a polynomial regression to N TDC consecutive measurements centered on the region of interest. In contrast with sub-nanosecond techniques, which are limited by the electronic time resolution[8], optoelectronic ADASOPS benefits from the stability of femtosecond oscillators, which is the key feature rendering a sub-picosecond time resolution achievable after averaging over a large number N of individual measurements.

The black sketch in Fig. 1(a) shows the optical setup associated with a practical implementation of optoelectronic ADASOPS. Laser 1 (MaiTai, Spectra-Physics) and Laser 2 (Vitesse, Coherent) are two commercial femtosecond oscillators, here integrated in femtosecond amplifiers (Hurricane, Spectra-Physics and Libra, Coherent). The oscillators have repetition rates equal respectively to 79.9 and 80.1 MHz, and are associated with the pump (Laser 1) and the probe (Laser 2). As in our previous experiments, the oscillators are free running, *i.e.* they are not locked to one another nor to a reference clock. Small fractions of the oscillator beams are transmitted through two optical fibers to the ADASOPS device, leaving most of the energy available for pump-probe experiments. The optical part of the setup is thus of utter simplicity, as most of the complexity is now confined to the specially-designed electronics, of which the functional diagram is shown in Fig. 1(b). The optical fibers are directly connected to two amplified photodetectors (HFD3180-203, Finisar) whose outputs are digitized by leading edge discriminators before being conditioned as trigger signals for the TDC Start and Stop commands. The TDC is embedded into a Time Measurement Unit

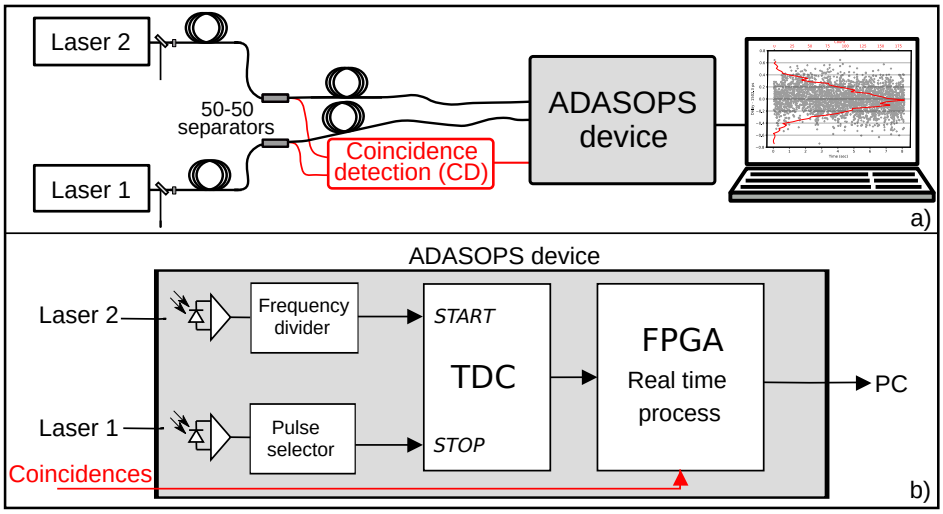

Figure 1: *(a) Optical setup. Elements drawn in black are the only components needed for optoelectronic ADASOPS. The additional coincidence detection setup shown in red is used to characterize the time resolution of the method. (b) Functional diagram of the components constituting the electronic ADASOPS device.*

(THS788, Texas Instrument), which is specified for a time measurement precision (LSB) of 13.02 ps. The TDC time-measurement temperature coefficient is 0.1 ps/°C, which is well compatible with the standard air-conditioning system of the lab (23°C±0.1°C). As the TDC is not able to directly sustain the high repetition rate of the oscillator, the Laser-2 signal is sent through a frequency divider in order to generate Start pulses separated by MT_2, with $M = 7$, corresponding to an effective measurement rate of $1/(MT_2) \approx 11.4$ MHz. Stop commands are triggered by the first Laser-1 pulse occurring after each Start pulse. In order to limit the noise, the electronic front-end has a 2.5-GHz bandwidth limit and includes differential transmission lines as well as a linear regulator power supply. A Field-Programmable Gate Array (FPGA) device (XC7A200T, Xilinx) drives the TDC operation and computes other experimental parameters such as laser repetition rates. Pulse counters are also connected to the Laser-1 and Laser-2 signals, the latter being used for generating a series of timestamps (corresponding to the integer i defined above) which are associated to each TDC measurement or other events. A FIFO (First In First Out)/USB3 bridge (FT600, FTDI Chip) sends the data stream to a personal computer (PC) where the polynomial regression is implemented.

3 Time resolution of TDC measurements

The standard deviation of TDC measurements can be readily evaluated by using a series of delays measured using the setup discussed in the previous section. Fig. 2 shows such a series of consecutive measurements. Note that it is not the pump-probe delay which is measured here but the probe-pump delay, as it is the probe signal (Laser 2) that triggers the TDC and sets the time origin. As expected, the measurement shows a typical sawtooth behavior, with a linear variation folded inside interval $[0, T_1]$. By differentiating the TDC measurement sequence, *i.e.* by computing the difference between consecutive measurements, we obtain two groups of values closely distributed around two quantities. The first and most common case corresponds to a positive quantity associated with the small increment between two consecutive measurements, whereas the second possibility occurs at each sawtooth jump and yields a negative quantity of large absolute value. Let us first concentrate on the former case, which is shown in Fig. 3(a) for a 1-ms acquisition period. It is noteworthy that the measured increments can only take discrete values separated by a multiple of the 13.02-ps TDC LSB unit. Figure 3(b) shows the corresponding histogram, which is in perfect agreement with a gaussian fit associated with a standard deviation of 12.0 ps. As this quantity results from the difference between two

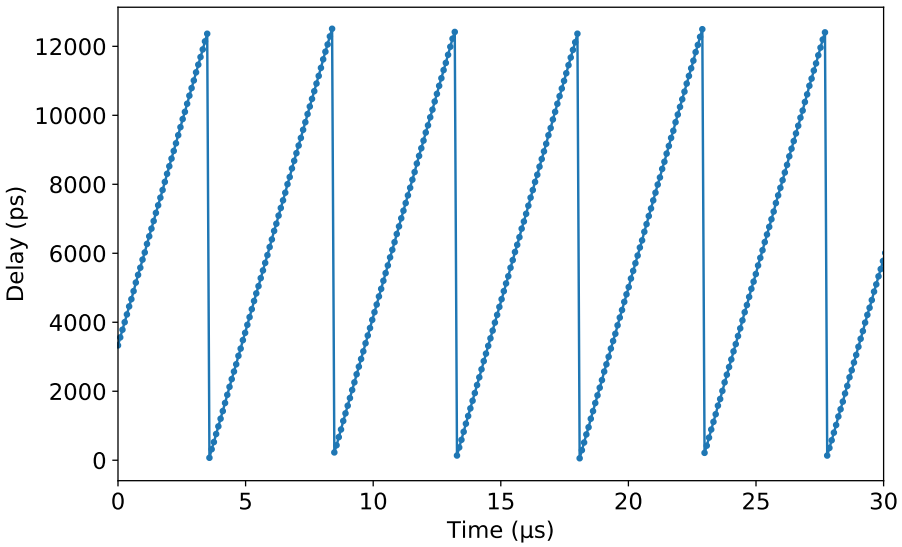

Figure 2: *Consecutive TDC values shown as a function of the time of measurement.*

consecutive measurements, each independently affected by the TDC dispersion, the result must be divided by $\sqrt{2}$ to yield the TDC standard deviation $R_{\rm tdc} \approx 12.0/\sqrt{2} \approx 8.5$ ps RMS. Figure 3(b) also illustrates the analogy with optical microscopy that we outlined above, with the discrete TDC values corresponding to the camera pixels and the gaussian time distribution corresponding to the microscope Point Spread Function (PSF) associated with the diffraction limit. As in optical microscopy, the gaussian center can be localized with excellent accuracy, equal to the gaussian width divided by $\sqrt{N}$.

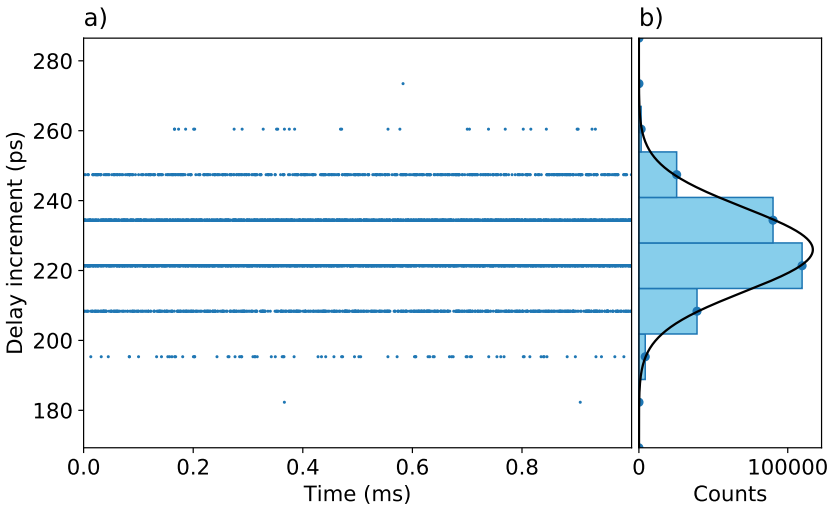

Figure 3: *(a) Difference between consecutive TDC measurements plotted as a function of time during a 1-ms acquisition time. The vertical scale has been set to show only the first group of data points associated with the smallest increment, as discussed in the text. (b) Histogram associated with a 50-msec acquisition time and gaussian fit corresponding to a center delay of 225.96 ps and a standard deviation of 12.0 ps.*

Considering the fact that the time elapsed between the probe and the pump increases by $(T_1 - T_2)$ for each pair of laser shots, and that the TDC measurement occurs every $M = 7$ pulses, the figure of approximately 225.96 ps thus obtained yields a very accurate estimate of the quantity $M \times (T_1 - T_2)$. Similarly, the other

group of data points corresponding to the sawtooth jump yields the quantity $M \times (T_1 - T_2) - T_1$, so that the two results taken together yield a very accurate determination of T_1 and T_2 in terms of TDC units. Conversely, as T_1 and T_2 can also be accurately determined by the FPGA from the counter inputs, these measurements can be used to provide an accurate determination of the TDC unit in our experimental conditions (including room temperature).

In order to confirm the TDC time resolution determined above, we performed an independent determination in the specific case where the pulses correspond to a coincidence between the two oscillators. For this purpose, we make use of the coincidence detection (CD) setup shown in red in Fig. 1(a). Indeed, in the way towards the ADASOPS device, half of each beam is redirected by 50:50 fiber separators to the CD setup, which consists of a fiber-based interferometer as described elsewhere[23]. To allow linear interference between the two beams (both centered at 800 nm), we use single mode fiber components in the entire setup. The output signal from the CD is connected to the ADASOPS device where coincidence events are processed by the FPGA and transmitted to the PC. The time resolution associated with the coincidence detection itself can be readily evaluated [23] and is found to be equal to 50 fs RMS in our present experimental conditions.

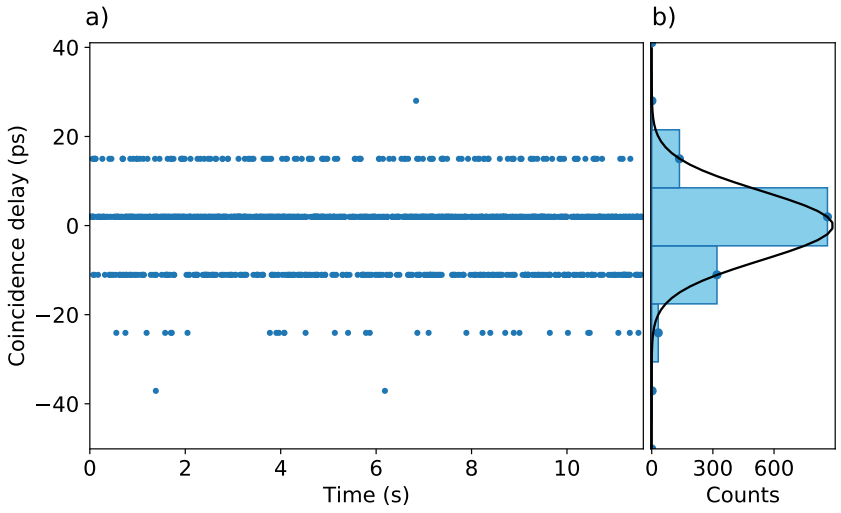

Figure 4: *(a) TDC measurements obtained for pulses corresponding to coincidences between pump and probe pulses. (b) Resulting histogram and gaussian fit corresponding to a standard deviation of 7.8 ps. A constant offset corresponding to the gaussian center has been subtracted from both graphs.*

Figure 4(a) shows a series of measured delays obtained when the coincidence events happened to occur at the same time as a TDC measurement (*i.e.* one seventh of all coincidence events). As the CD selects pairs of pulses that coincide at the interferometer level, there is a constant offset in the delay measured by the TDC corresponding to the overall optical and electronic path difference toward the TDC between lasers 1 and 2. This offset (which was equal to 2998.85 ps) is of no interest and has been subtracted from the data shown in Fig. 4. Again, the plot clearly shows a quantification of the TDC values. The histogram shown in Fig. 4(b) is in excellent agreement with a gaussian fit of standard deviation 7.8 ps. This independent determination of R_{tdc} is in good agreement with the previous method. The slight overestimation observed in the previous method might be attributed to the fact that it is sensitive to fluctuations of the cavity lengths, unlike the direct comparison with coincidences. In the following, we will use the estimate $R_{\mathrm{tdc}} \approx 8$ ps.

4 Demonstration of optoelectronic ADASOPS

We now apply the procedure outlined in section 2 and use a regression algorithm with N unwrapped consecutive TDC measurements, that we choose centered on each detected coincidence for validation purpose. From the obtained polynomial coefficients combined with eq. 1, we can compute the pump-probe delay for all pulse pairs. In contrast with the approach used in the previous section, the delay can thus be computed for all coincidence events, even those which did not raise a TDC measurement but were among the $M-1$ skipped pulses. The associated values (after offset subtraction) are drawn as blue crosses in Fig. 5(a) for an optimal choice of parameters, which corresponds here to a 4^{th}-order polynomial fit over $N = 16384$ TDC measurements. Unlike the raw TDC measurements, the obtained pattern does not suffer from discretization and is finely distributed over a narrow gaussian distribution, as shown with the superimposed histogram. The associated standard deviation is found to be as good as 200 fs. This value corresponds to the convolution of the optoelectronic ADASOPS resolution and that of coincidence detection. As the measured value is significantly larger than the 50-fs standard deviation mentioned above for coincidence detection, it can be considered to be a good estimate of the actual dispersion of our new method.

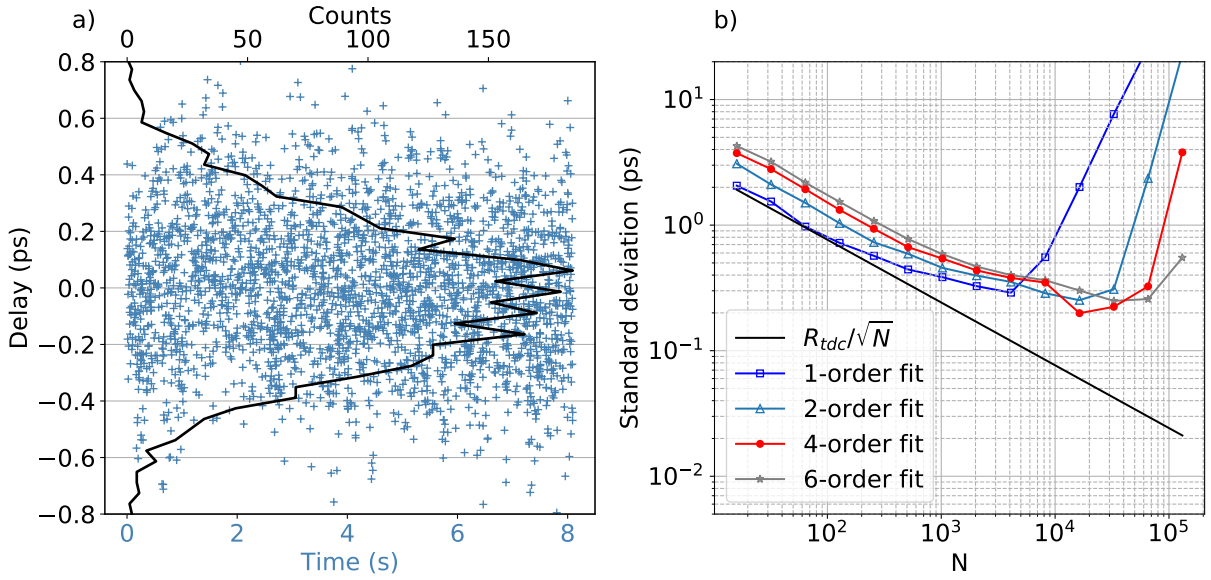

Figure 5: *(a) Series of time delays (blue crosses) computed for pulse pairs associated with coincidence detection, with $N = 2^{14} = 16384$ and $n = 4$, superimposed with the corresponding histogram (black solid line). (b) Measured standard deviation plotted in log-log scale as a function of N for polynomial regressions of orders $n = 1, 2, 4$ and 6. The black solid line corresponds to the $R_{\text{tdc}}/\sqrt{N}$ limit.*

Figure 5(b) shows, in log-log scale, a comparative study evidencing the effect on the measured standard deviation of two different parameters: the number of TDC measurements, N, and the degree of the polynomial, n. We observe the expected $1/\sqrt{N}$ behavior for small N values (typically $N \leq 64$). In this region the first-order polynomial is beneficial, as there are fewer coefficients p_k to determine from a given amount of experimental data. An optimum value is then obtained for greater N values, before the standard deviation worsens up for even greater N values. The departure from the $1/\sqrt{N}$ law can be interpreted by remarking that for large N values the averaging duration, MNT_2, will become comparable with the characteristic timescale of the cavity drift, so that the hypothesis of a still cavity breaks down. In other words, the hypothesis that the errors on different TDC measurements are independent random variables breaks down, and so does the $1/\sqrt{N}$ law. The optimum found in the case of linear regression ($N = 4096$) yields a characteristic time

$MNT_2 \approx 0.36$ ms, which is consistent with our previous experience on coincidence-based ADASOPS [24]. In contrast, a fourth-order polynomial manages to track the cavity drift properly (at least at the lowest order) for a longer duration corresponding here to $N = 2^{14} = 16384$. As a consequence, the standard deviation is smaller, which yields the optimal conditions shown in Fig. 5(a). In case of kHz-ADASOPS[25], note that the optimal averaging time is not related to the repetition rate of the amplifier but only to the dynamics of the oscillator cavity.

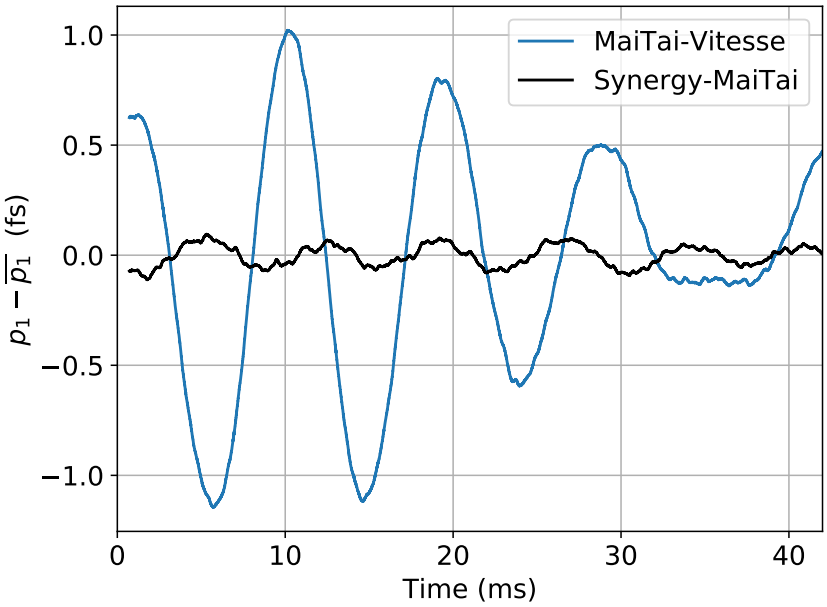

Figure 6: *Typical evolution of the p_1 coefficient determined from a sliding 4^{th} order fit with $N = 16384$, after subtraction of the average value, $\overline{p_1}$. The blue (resp. black) solid line shows the measurement obtained with a MaiTai-Vitesse (resp. Synergy-MaiTai) oscillator pair.*

In order to illustrate the importance of the cavity dynamics, we plot in Fig. 6 an example of time variation of the coefficient p_1 as obtained from a series of sliding fourth-order regressions (blue curve). This coefficient corresponds to the slope of the delay law, $T_1 - T_2$, and thus directly reflects the change in cavity length. We observe an oscillatory behavior suggesting mechanical vibrations, that we attribute to the chiller units connected to the Titanium:Sapphire crystals. Indeed, by replacing the integrated Vitesse oscillator with a standalone Synergy (Femtolaser) oscillator, we obtain a much smaller variation of the same coefficient (black curve). The greater cavity fluctuation observed for the Vitesse can be attributed to the fact that it is connected to a 2200-W chiller, which also regulates the 4-W Libra amplifier, whereas the MaiTai and Synergy oscillators are cooled by chillers of respective powers equal to only 700 and 250 W. The vibration frequency of about 100 Hz is also compatible with the mechanical noise generated in the cooling unit, as was confirmed by a 100-Hz peak observed in the Fourier spectrum of the acoustic noise recorded near the chiller. Although the 1-fs amplitude observed in Fig. 6 may not seem like much at first sight, the resulting error accumulation in eq. 1 explains the large increase of the standard deviation observed in Fig. 5(b) for large N values, in case of a linear fit. In contrast, the fourth-order fit succeeds in capturing the cavity oscillation, hence increasing the optimal N value and decreasing the standard deviation thus achieved.

5 Summary

To summarize, we have demonstrated a new ADASOPS method based on electronic rather than interferometric detection of the time delays between oscillator pulse pairs. The poorer time resolution of the electronics, measured to be approximately 8 ps RMS, is compensated for by the large acquisition rate, set to 11.4 MHz in our experiment. By appropriate averaging and using a fourth-order polynomial fit, we demonstrate that the time delay between each pair of pulses can be predicted with a time resolution as good as 200 fs RMS. The new method is associated with a very simple optical setup and offers several key advantages. Unlike the interferometric approach, there is no need for a spectral overlap between the two oscillators, provided that appropriate photodetectors are used for each laser. This feature makes the method more versatile and suitable for a greater variety of different femtosecond oscillators, including fibered oscillators which emit in different spectral domains. The higher acquisition rate allows us to keep track of rapid drift in cavity lengths, as caused by vibrations induced by chillers common in integrated femtosecond amplifiers. Optoelectronic ADASOPS can thus be readily combined with multiscale control and rapid scanning of time delays up to millisecond timescales [25]. Finally, the higher TDC acquisition rate will be of great interest when a long-cavity oscillator is used as the pump laser, in which case the low coincidence rate was so far the main factor limiting the time resolution[14].

Funding

LabEx PALM ("Investissement d'avenir" program ANR-10-LABX-0039-PALM).

Acknowledgments

We wish to thank Alexis Jeandet, Janette Trayaud and Marten H. Vos for fruitful discussions.

Disclosures

L.A., X.S., A.B. and M.J. are authors of a patent (P) describing the general principle of ADASOPS (FR1155799, US10190972B2).

References

[1] B. Lang, "Photometrics of ultrafast and fast broadband electronic transient absorption spectroscopy: State of the art," Rev. Sci. Instr. **89**, 093112 (2018).

[2] G. Sucha, M. E. Fermann, D. J. Harter, and M. Hofer, "A new method for rapid temporal scanning of ultrafast lasers," IEEE J. Sel. Top. Quant. Electr. **2**, 605–621 (1996).

[3] E. Lill, S. Schneider, and F. Dorr, "Rapid optical sampling of relaxation-phenomena employing 2 time-correlated picosecond pulsetrains," Appl. Phys. **14**, 399–401 (1977).

[4] P. A. Elzinga, F. E. Lytle, Y. Jian, G. B. King, and N. M. Laurendeau, "Pump probe spectroscopy by asynchronous optical-sampling," Appl. Spectrosc. **41**, 2–4 (1987).

[5] J. D. Kafka, J. W. Pieterse, and M. L. Watts, "2-color subpicosecond optical-sampling technique," Opt. Lett. **17**, 1286–1288 (1992).

[6] F. Keilmann, C. Gohle, and R. Holzwarth, "Time-domain mid-infrared frequency-comb spectrometer," Opt. Lett. **29**, 1542–1544 (2004).

[7] R. Gebs, G. Klatt, C. Janke, T. Dekorsy, and A. Bartels, "High-speed asynchronous optical sampling with sub-50fs time resolution," Opt. Express **18**, 5974–5983 (2010).

[8] T. Nakagawa, K. Okamoto, H. Hanada, and R. Katoh, "Probing with randomly interleaved pulse train bridges the gap between ultrafast pump-probe and nanosecond flash photolysis," Opt. Lett. **41**, 1498–1501 (2016).

[9] H. R. Ma, J. Ervin, and M. Gruebele, "Single-sweep detection of relaxation kinetics by submicrosecond midinfrared spectroscopy," Rev. Sci. Instr. **75**, 486–491 (2004).

[10] M. Byrdin, V. Thiagarajan, S. Villette, A. Espagne, and K. Brettel, "Use of ruthenium dyes for subnanosecond detector fidelity testing in real time transient absorption," Rev. Sci. Instrum. **80**, 043102 (2009).

[11] J. Bredenbeck, J. Helbing, J. R. Kumita, G. A. Woolley, and P. Hamm, "Alpha-helix formation in a photoswitchable peptide tracked from picoseconds to microseconds by time-resolved ir spectroscopy," Proc. Natl. Acad. Sci. USA **102**, 2379–2384 (2005).

[12] M. M. Leonova, T. Y. Fufina, L. G. Vasilieva, and V. A. Shuvalov, "Structure-function investigations of bacterial photosynthetic reaction centers," Biochemistry (Mosc) **76**, 1465–1483 (2011).

[13] B.-K. Yoo, I. Lamarre, F. Rappaport, P. Nioche, C. S. Raman, J.-L. Martin, and M. Negrerie, "Picosecond to second dynamics reveals a structural transition in clostridium botulinum no-sensor triggered by the activator bay-41-2272," ACS Chem. Biol. **7**, 2046–2054 (2012).

[14] L. Antonucci, A. Bonvalet, X. Solinas, M. R. Jones, M. H. Vos, and M. Joffre, "Arbitrary-detuning asynchronous optical sampling pump-probe spectroscopy of bacterial reaction centers," Opt. Lett. **38**, 3322–3324 (2013).

[15] P. E. Konold, I. H. M. van Stokkum, F. Muzzopappa, A. Wilson, M.-L. Groot, D. Kirilovsky, and J. T. M. Kennis, "Photoactivation mechanism, timing of protein secondary structure dynamics and carotenoid translocation in the orange carotenoid protein," J. Am. Chem. Soc. **141**, 520–530 (2019).

[16] L. Martinez-Fernandez, P. Changenet, A. Banyasz, T. Gustavsson, D. Markovitsi, and R. Improta, "Comprehensive study of guanine excited state relaxation and photoreactivity in g-quadruplexes," J. Phys. Chem. Lett. **10**, 6873–6877 (2019).

[17] J. Bredenbeck, J. Helbing, and P. Hamm, "Continuous scanning from picoseconds to microseconds in time resolved linear and nonlinear spectroscopy," Rev. Sci. Instr. **75**, 4462–4466 (2004).

[18] A. C. Yu, X. Ye, D. Ionascu, W. X. Cao, and P. M. Champion, "Two-color pump-probe laser spectroscopy instrument with picosecond time-resolved electronic delay and extended scan range," Rev. Sci. Instr. **76**, 114301 (2005).

[19] G. M. Greetham, D. Sole, I. P. Clark, A. W. Parker, M. R. Pollard, and M. Towrie, "Time-resolved multiple probe spectroscopy," Rev. Sci. Instr. **83**, 103107 (2012).

[20] T. Mathes, J. Ravensbergen, M. Kloz, T. Gleichmann, K. D. Gallagher, N. C. Woitowich, R. St Peter, S. E. Kovaleva, E. A. Stojkovic, and J. T. M. Kennis, "Femto- to microsecond photodynamics of an unusual bacteriophytochrome," J. Phys. Chem. Lett. **6**, 239–243 (2015).

[21] G. M. Greetham, P. M. Donaldson, C. Nation, I. V. Sazanovich, I. P. Clark, D. J. Shaw, A. W. Parker, and M. Towrie, "A 100 khz time-resolved multiple-probe femtosecond to second infrared absorption spectrometer," Appl. Spectrosc. **70**, 645–653 (2016).

[22] Y. Song, A. Konar, R. Sechrist, V. P. Roy, R. Duan, J. Dziurgot, V. Policht, Y. A. Matutes, K. J. Kubarych, and J. P. Ogilvie, "Multispectral multidimensional spectrometer spanning the ultraviolet to the mid-infrared," Rev. Sci. Instr. **90**, 013108 (2019).

[23] L. Antonucci, X. Solinas, A. Bonvalet, and M. Joffre, "Asynchronous optical sampling with arbitrary detuning between laser repetition rates," Opt. Express **20**, 17928–17937 (2012).

[24] L. Antonucci, A. Bonvalet, X. Solinas, L. Daniault, and M. Joffre, "Arbitrary-detuning asynchronous optical sampling with amplified laser systems," Opt. Express **23**, 27931–27940 (2015).

[25] X. Solinas, L. Antonucci, A. Bonvalet, and M. Joffre, "Multiscale control and rapid scanning of time delays ranging from picosecond to millisecond," Opt. Express **25**, 17811–17819 (2017).

[26] R. E. Thompson, D. R. Larson, and W. W. Webb, "Precise nanometer localization analysis for individual fluorescent probes," Bioph. J. **82**, 2775–2783 (2002).